Neurobiology of Aging 79 (2019) 30–42

Contents lists available at ScienceDirect

Neurobiology of Aging

journal homepage: www.elsevier.com/locate/neuaging

Modulation of miR-34a/SIRT1 signaling protects cochlear hair cells against oxidative stress and delays age-related hearing loss through coordinated regulation of mitophagy and mitochondrial biogenesis

Hao Xiong [1], Suijun Chen [1], Lan Lai [1], Haidi Yang [1], Yaodong Xu, Jiaqi Pang, Zhongwu Su, Hanqing Lin, Yiqing Zheng*

Department of Otolaryngology, Sun Yat-sen Memorial Hospital, Sun Yat-sen University, Guangzhou, China
Institute of Hearing and Speech-Language Science, Sun Yat-sen University, Guangzhou, China

ARTICLE INFO

Article history:
Received 4 December 2018
Received in revised form 14 March 2019
Accepted 21 March 2019
Available online 27 March 2019

Keywords:
Mitophagy
Mitochondrial biogenesis
Cochlea
Presbycusis
SIRT1
Oxidative stress

ABSTRACT

Mitophagy and mitochondrial biogenesis are 2 pathways that regulate mitochondrial content and metabolism maintaining cellular homeostasis. The imbalance between these opposing processes impairs mitochondrial function and is suggested to be the pathophysiological basis of a variety of neurodegenerative diseases and aging. Here we investigated the role of mitophagy and mitochondrial biogenesis in oxidative damage to the cochlear hair cells and age-related hearing loss. In cultured mouse House Ear Institute-Organ of Corti 1 hair cells, oxidative stress activated mitophagy but inhibited mitochondrial biogenesis and impaired mitochondrial function. Pharmacological inhibition of miR-34a/SIRT1 signaling enhanced mitophagy, mitochondrial biogenesis, and attenuated House Ear Institute-Organ of Corti 1 cell death induced by oxidative stress. In the cochlea of C57BL/6 mice, mitophagy and mitochondrial biogenesis were both upregulated during aging. Long-term supplementation with resveratrol, a SIRT1 activator, not only improved the balance between mitophagy and mitochondrial biogenesis but also significantly reduced age-related cochlear hair cell loss, spiral ganglion neuron loss, stria vascularis atrophy, and hearing threshold shifts in C57BL/6 mice. Moreover, SIRT1 overexpression or miR-34a deficiency both attenuated age-related cochlear hair cell loss and hearing loss in C57BL/6 mice. Our findings reveal that imbalance between mitophagy and mitochondrial biogenesis contributes to cochlea hair cell damage caused by oxidative stress and during aging. Coordinated regulation of these 2 processes by miR-34a/SIRT1 signaling might serve as a promising approach for the treatment of age-related cochlear degeneration and hearing loss.

1. Introduction

Age-related hearing loss (AHL) is the most common form of hearing loss and the predominant age-related neurodegenerative disease (Gates and Mills, 2005). AHL is prevalent in nearly two-thirds of adults aged 70 years or older, which can lead to social isolation, major communication difficulties, and decreased physical function (Homans et al., 2017; Wilson et al., 2017). AHL is likely a multifactorial condition which results from the coactions of genetic predisposition and a lifetime of insults to the ear including exposure to noise and ototoxic chemicals (Bielefeld et al., 2010; Yamasoba et al., 2013). Currently, it is well known that the irreversible loss of cochlear hair cells in the inner ear is a key contributor in the pathogenesis of AHL. Despite considerable efforts, the mechanisms underlying AHL are not well understood and there are still no FDA-approved drugs to treat AHL so far.

Mitochondria are highly dynamic organelles and essential for energy production and cellular homeostasis. The precise regulation of mitochondrial mass, distribution, and activity is extremely crucial for maintenance of cellular homeostasis. A shared hallmark of a variety of age-related pathological conditions and aging is impaired mitochondrial function and deregulation of cellular mitochondrial content (Lopez-Otin et al., 2013). Maintenance of mitochondrial function requires both generation of newly

* Corresponding author at: Department of Otolaryngology, Sun Yat-sen Memorial Hospital, Institute of Hearing and Speech-Language Science, Sun Yat-sen University, 107 West Yan Jiang Road, Guangzhou 510120, China. Tel.: +86-20-81332566; fax: +86-20-81332115.
E-mail address: zhengyiq@mail.sysu.edu.cn (Y. Zheng).
[1] These authors contributed equally to this work.

0197-4580/$ – see front matter © 2019 Elsevier Inc. All rights reserved.
https://doi.org/10.1016/j.neurobiolaging.2019.03.013

synthesized mitochondria and removal of dysfunctional mitochondria, termed mitochondrial biogenesis and mitophagy, respectively. Mitochondrial biogenesis is a complex process, including mtDNA transcription and translation, translation of nucleus-derived transcripts, recruitment of newly synthesized proteins and lipids, mitochondrial import and assembly of the oxidative phosphorylation complexes (Zhu et al., 2013). On the contrary, mitophagy is a multistep process that involves the targeting of damaged or superfluous mitochondria to the lysosomes, where these mitochondria are degraded (Fang et al., 2014; Palikaras et al., 2015b). Recent findings hint that mitophagy and mitochondrial biogenesis are tightly coupled, and imbalance between the 2 processes correlated with many human pathologies and aging (Andres et al., 2015; Palikaras et al., 2015a). However, the cellular and molecular mechanisms underlying the interplay and modulation between mitophagy and mitochondrial biogenesis remain obscure.

MicroRNAs (miRNAs) are approximately 20–24 nt noncoding RNAs that direct post-transcriptional repression of mRNA targets in human and other mammals (Bartel, 2018). Recently, miRNAs were observed in the cochlea and suggested to play a crucial role in AHL (Patel and Hu, 2012; Zhang et al., 2013). Nevertheless, the role of miRNAs in determining the fate of cochlear hair cells during AHL pathogenesis has not been fully elucidated. Of interest is miR-34a, which has been implicated as a key player inducing multiple age-related pathologies and aging (Boon et al., 2013; Guo et al., 2017; Liu et al., 2012). Intriguingly, our previous studies have demonstrated that miR-34a targets SIRT1 and correlates with age-related cochlear hair cell loss and AHL (Xiong et al., 2014, 2015). However, how miR-34a/SIRT1 signaling causes cochlear degeneration during aging remains elusive. SIRT1 is one of the sirtuins of NAD^+-dependent deacetylases that mediate the health benefits and longevity, possibly through maintenance of mitochondrial homeostasis (Herskovits and Guarente, 2014; Mouchiroud et al., 2013; Price et al., 2012). Recently, SIRT1 has been strongly implicated in the modulation of mitophagy and mitochondrial biogenesis through its downstream targets (Di Sante et al., 2015; Fang et al., 2014; Tang, 2016; Zaini et al., 2018).

In this study, we tested mitophagy and mitochondrial biogenesis in conditionally immortalized mouse auditory cells (House Ear Institute-Organ of Corti 1 [HEI-OC1] cells) on challenge with oxidative stress, which mimics the condition that in aging cochlea. In addition, we examined the efficiency of modulation of miR-34a/SIRT1 signaling in the improvement of HEI-OC1 cell survival under oxidative stress. Moreover, we also monitored mitophagy and mitochondrial biogenesis and their modulation by miR-34a/SIRT1 signaling in the cochlea of C57BL/6 mice, a well-established mouse model of AHL.

2. Materials and methods

2.1. Animals and diets

C57BL/6 mice were purchased from The Laboratory Animal Center, Sun Yat-sen University (Guangzhou, China). miR-34a$^{+/-}$ mice and SIRT1 transgenic (Tg) mice on the C57BL/6 background were obtained from Cyagen Biosciences Inc (Guangzhou, China). C57BL/6 mice were randomly divided into 5 groups: a "young" group (2 months of age), an "old" group (12 months of age), and 3 "old + treatment" groups. In the treatment groups, mice were subject to dietary supplementation with 7.5 or 300 mg/kg/d resveratrol (100 or 4000 mg resveratrol/kg of food, Sigma-Aldrich) or 14 mg/kg/d rapamycin (200 mg rapamycin/kg of food, Selleck) added to the chow for a period of 10 months from 2 months of age, whereas the "old group" only fed standard chow.

2.2. Auditory brainstem response

All mice were anesthetized with an intraperitoneal injection (100 mg/kg ketamine and 10 mg/kg xylazine mixture), and auditory brainstem response (ABR) measurements performed by inserting subdermal needle electrodes at the vertex (active), under the left ear (reference), and under the right ear (ground). The acoustic signals were generated, and the responses were processed using Tucker-Davis Technologies (TDT System III, Alachua, FL, USA) hardware and software. Ten millisecond (ms) tone bursts with a 1 ms rise/fall time were presented at 8, 16, and 32 kHz at a rate of 21.1/s. The average response to 1000 stimuli was obtained by reducing the sound intensity at 5 dB intervals near the threshold, which was defined as the lowest stimulation decibel level at which a positive wave in the evoked response trace was evident.

2.3. Tissue preparation

After ABR recordings, the deeply anesthetized mice were decapitated and the cochleae removed and fixed by immersion in 4% paraformaldehyde in 0.1 mM phosphate-buffered saline (PBS, pH 7.4) overnight at 4 °C. The cochleae were decalcified in 4% sodium ethylenediaminetetraacetic acid for 4 days followed by an overnight incubation in 30% sucrose. The next day, some cochleae were embedded in O.C.T. (Sakura), cryosectioned at a 10-μm thickness, and stored at -20 °C for immunohistochemistry. Some cochleae were embedded with paraffin and sliced at a 5-μm thickness for staining with hematoxylin and eosin. Some cochleae were directly processed for surface preparations. For RNA and protein preparations, cochlear tissues were dissected with small forceps, snap frozen in liquid nitrogen, and stored at −80 °C.

2.4. Surface preparations for hair cell counts

After decalcification with ethylenediaminetetraacetic acid, some cochleae were permeabilized with 0.3% Triton X in PBS for 30 minutes and stained with Alexa Fluor 488 phalloidin at 1:200 (Thermo Fisher Scientific) for 30 minutes. After rinsing with PBS, each cochlea was microdissected into apical, middle, and basal segments, and the tissues were mounted on glass slides in 50% glycerol. Cochlear samples were observed and imaged with an Olympus BX63 microscope. Hair cells, including outer hair cells (OHCs) and inner hair cells (IHCs), were counted from the apex to the base along the entire length of the cochlear epithelium. The percentage of hair cell loss in each 0.5 mm length of epithelium was plotted versus cochlear length as a cytocochleogram.

2.5. Spiral ganglion neuron counts

Spiral ganglion neurons (SGNs, types I and II) in Rosenthal's canal in the middle turn were counted in cochlear sections stained with hematoxylin and eosin. The cells were identified by the presence of a nucleus. Data were averaged from 3 images for each mouse. The SGN survival was calculated as the number of cells per mm^2.

2.6. Stria vascularis thickness measurements

Stria vascularis thickness measurements were taken from cochlear sections stained with hematoxylin and eosin. Measurements were made in 3 images containing the middle turn of the cochlea for each mouse and data were pooled to obtain a mean. Stria vascularis thickness was defined as the distance between the margin of the stria vascularis to the junction of the basal cells at the central portion of the stria vascularis width (along the axis of Reissner's membrane to spiral prominence).

2.7. Immunohistochemistry of cochlear surface preparations and cryosections

The detailed procedures of immunohistochemistry were described in our previous study (Xiong et al., 2017). In brief, cochlear sections or whole mounts were incubated overnight at 4 °C with polyclonal rabbit anti-Myosin at 1:200 (Santa Cruz, sc74516), monoclonal mouse anti-PGC-1α at 1:100 (Abcam, ab54481), monoclonal mouse anti-NRF1 at 1:100 (Abcam, ab175932), monoclonal mouse anti-NRF2 (Abcam, ab62352), monoclonal mouse anti-PINK1 at 1:100 (Abcam, ab75487), monoclonal mouse anti-TOMM20 at 1:100 (Santa Cruz, sc17764), polyclonal rabbit anti-4HNE at 1:200 (Abcam, ab46545), and monoclonal rabbit anti-CtBP2 at 1:200 (BD Biosciences, 612044). After several washes, samples were incubated with Alexa flour 594 secondary antibodies (Invitrogen) at 1:200 at room temperature for 1 hour and counterstained with Alexa Fluor 488 phalloidin at 1:200 and 4′,6-diamidino-2-phenylindole (DAPI) (10 mg/mL, Sigma-Aldrich). Cochlear samples were observed and imaged with a Zeiss LSM 710 confocal microscope.

2.8. Quantification of immunolabeled signals from cochlear surface preparations

We quantified immunolabeled signals from surface preparations using a protocol that has been described previously (Xiong et al., 2017). Briefly, immunolabeled signals of OHCs in surface preparations were quantified from original confocal images. Each image was taken with a 63× magnification lens under identical conditions and with equal parameter settings for laser gains and photomultiplier tube gains using ImageJ software (National Institutes of Health). Cochlear samples from the different groups were fixed and stained simultaneously with identical solutions and processed in parallel. All surface preparations were counterstained with phalloidin or DAPI for labeling OHC structure to identify comparable parts of OHCs in confocal images. Immunofluorescence was measured in the upper basal turn (22–32 kHz region) of cochlear surface preparations in 0.12 mm segments, each containing about 60 OHCs. The intensity of the background fluorescence was subtracted, and the average fluorescence per cell was then calculated. Relative fluorescence was quantified by normalizing the ratio of average fluorescence of aging hair cells to that from young controls.

2.9. HEI-OC1 cell culture and oxidative stress exposure

HEI-OC1 cells (kindly provided by F. Kalinec at the House Ear Institute, Los Angeles, CA, USA) were cultured in Dulbecco's modified Eagle's medium (Gibco), supplemented with 10% fetal bovine serum (Gibco) at 33 °C under 10% CO2 (permissive conditions). For in vitro oxidative stress test, HEI-OC1 cells were exposed to H_2O_2 at 1 mM for indicated hours for a does-dependent analysis. For cell viability analysis, HEI-OC1 cells were pretreated with different agents for 12–24 hours and then exposed to H_2O_2 at 1 mM for 1 hour. The selection of H_2O_2 concentration is based on our own preliminary results (data not shown).

2.10. GFP-LC3–labeled HEI-OC1 cell production

The HEI-OC1 cells were transfected with lentivirus-mediated green fluorescent protein (GFP)-LC3 to generate GFP-LC3–expressing cells. The lentivirus containing GFP-LC3 fusion genes were purchased from Hanbio Biotechnology (Shanghai, China). HEI-OC1 cells were plated into 6-well dishes and infected with the recombinant lentivirus following the manufacturer's instructions. After 48 hours, cells were selected by culture in the presence of puromycin for 2 weeks. Cells stably transfected with GFP-LC3 were counterstained with MitoTracker under normal or H_2O_2 treatment conditions.

2.11. Immunocytochemistry in the HEI-OC1 cells

Cultured HEI-OC1 cells were fixed with 4% paraformaldehyde for 30 minutes and incubated overnight at 4 °C with monoclonal mouse anti-PINK1 at 1:200 (Abcam, ab75487) or monoclonal mouse anti-LAMP1 at 1:200 (Abcam, ab119127). Cultures were then incubated with mitochondrial probe MitoTracker Red CMXRos (Yeasen) for 1 hour. Samples were then counterstained with DAPI for 30 minutes and imaged with an Olympus BX63 microscope.

2.12. Quantitative real-time polymerase chain reaction

Total RNA was isolated using TRIzol Reagent (Invitrogen) according to the manufacturer's protocol, with 1 μg of total RNA reverse-transcribed using a ReverTra-Plus-TM kit (Toyobo). Primer sequences used for amplifications were as follows: SIRT1 forward: 5′-CGGCTACCGAGGTCCATATAC-3′, reverse: 5′-ACAATCTGCCACAGCGTCAT-3′. cDNA samples were amplified using SYBR Premix Ex Taq (Takara) and detected with the Roche LightCycler 480 real-time polymerase chain reaction system. GAPDH was used as internal control for SIRT1 normalization. For miR-34a expressional analysis, enriched small RNAs were isolated from cochlear tissues using TRIzol reagent, with 500 ng of RNA reverse-transcribed using specific miRNA stem-loop primers and a PrimeScript RT reagent Kit (Takara). Mature miRNA expression was measured with Takara Taq Version 2.0 plus dye (Takara) according to the manufacturer's instructions, with miRNA levels normalized to U6 snRNA expression.

2.13. Western blotting analysis

Cochlear tissues and cultured cells were homogenized on ice-cold radioimmunoprecipitation assay lysis buffer (Thermo plus) for 30 minutes, centrifuged at 12,000 × *g* at 4 °C for 10 minutes and the supernatants collected. Protein concentrations were determined using a Protein Assay dye reagent (Bio-Rad). Protein samples (50 μg) were resolved via sodium dodecyl sulfate–polyacrylamide gel electrophoresis, with proteins transferred onto a polyvinylidene fluoride membrane (Millipore) and blocked with 5% nonfat dry milk in PBS with 0.1% Tween 20. The membranes were incubated with monoclonal mouse anti-SIRT1 (Abcam, ab110304), monoclonal mouse anti-PGC-1α (Abcam, ab54481), monoclonal mouse anti-TFAM (Abcam, ab131607), monoclonal mouse anti-NRF1 (Abcam, ab175932), monoclonal mouse anti-NRF2 (Abcam, ab62352), monoclonal mouse anti-PINK1 (Abcam, ab75487), monoclonal mouse anti-TOMM20 (Santa Cruz, sc17764), polyclonal rabbit anti-COX4 (Cell signaling, 4850S), polyclonal rabbit anti-4HNE (Abcam, ab46545), polyclonal rabbit anti-SOD1 (Proteintech, 10269-1-AP), polyclonal rabbit anti-LC3A/B (Cell Signaling, 12741S), and polyclonal rabbit anti-p62 (Cell Signaling, 5114S) at 1:1000 overnight, washed 3 times (10 minutes each) with PBS with 0.1% Tween 20, and incubated with an appropriate secondary antibody (1:10,000) for 1 hour. After extensive membrane washing, the immunoreactive bands were visualized by enhanced chemiluminescence (Millipore). Band intensities were quantified by densitometric analysis using NIH ImageJ, and glyceraldehyde-3-phosphate dehydrogenase was used as a loading and internal control to enable sample normalization.

2.14. Cell viability assay

An MTS assay [3-(4, 5-dimethylthiazol-2-yl)-5-(3-carboxymethoxyphenyl)-2-(4-sulfophenyl)-2H-tetrazolium, inner salt]

was performed to examine cell viability. HEI-OC1 cells in 100 μL of culture medium were exposed to 20 μL of CellTiter 96 Aqueous One Solution Assay (Promega) for 3 hours according to the manufacturer's instructions and quantified at an absorbance of 490 nm using a WELLSCAN MK3 microplate reader (Labsystems).

2.15. Mitochondrial DNA copy number analysis

Total DNA was extracted from 100 mg of cochlear tissue or cells cultured in 6-well plate using QIAamp DNA Mini kit (Qiagen). Mitochondrial DNA copy number was determined by amplifying genes encoded by mitochondrial DNA and genomic DNA. Total genomic DNA was extracted from cells using a Universal Genomic DNA Extraction Kit (Takara) according to the manufacturer's protocols. The mtDNA levels were quantified by quantitative real-time polymerase chain reaction on a Roche LightCycler 96 (Roche) using D-loop primers (forward: 5′-GGTTCTTACTTCAGGGCCATCA-3′, reverse: 5′-GATTAGACCCGTTACCATCGAGAT-3′). Nuclear gene beta2-microglobulin primers (forward: 5′-ATGGGAAGCCGAACATACTG-3′, reverse: 5′- CAGTCTCAGTGGGGGTGAAT-3′) were used as a nuclear control. Relative quantification of mitochondrial DNA copy number was calculated after using $2^{\Delta Ct}$ as fold change.

2.16. Mitochondrial membrane potential measurement

The mitochondrial membrane potential was measured with JC-1 fluorescent dye. JC-1 displays red or green fluorescent in a potential-dependent manner. Mitochondria with normal membrane potential take in JC-1 exhibit red fluorescent, whereas damaged mitochondria exhibit green fluorescent. The HEI-OC1 cells were stained with JC-1 in culture media for 15 minutes in culture condition and then washed with PBS 3 times. Mitochondrial membrane potential was detected by flow cytometry (BD Biosciences). The percentage of green fluorescent reflects damage mitochondrial membrane potential.

2.17. Mitochondrial reactive oxygen species detection

Mitochondrial reactive oxygen species (ROS) levels were measured by staining with MitoSOX (Molecular Probes) following the manufacturer's instructions. Briefly, cells were incubated with MitoSOX (5 μM) for 30 minutes at 37 °C. After being washed with PBS, the cells were counterstained with DAPI for 10 minutes and imaged with an Olympus BX63 microscope (Olympus).

2.18. Measurement of ATP levels

Adenosine triphosphate (ATP) assay was performed using an ATP Assay Kit (Beyotime, Shanghai, China) following the manufacturer's instructions. Briefly, cells were homogenized with lysis buffer and centrifuged at 12,000 × *g* for 5 minutes at 4 °C. ATP detection reagent was diluted with dilution buffer and added into 96-wells. Then samples were added into wells and mixed with detection solution. Chemiluminescence of samples and standards were measured with a SpectraMax M5 microplate reader (Molecular Devices). The levels of ATP were calculated based on the standard curve and normalized to the protein content.

2.19. Gene silencing

HEI-OC1 cells were transfected with a siRNA targeted to mouse Parkin (siParkin), PGC-1α (siPGC-1α), or Drp1 (siDrp1) and scrambled siRNA (Ruibo) according to manufacturer's instructions. After 24 hours of incubation, the expression of Parkin and PGC-1α protein was examined by Western blotting. For cell viability analysis, HEI-OC1 cells were transfected with siParkin, siPGC-1α, or siDrp1 for 24 hours, followed by exposure to H_2O_2 at 1 mM for 1 hour.

2.20. Statistic analysis

Data were presented as means ± SD and analyzed using IBM SPSS Statistics Premium V21. One-way ANOVA with Fisher post hoc test, Student's *t*-test and one sample *t*-tests were performed for statistical analysis. Values of $p < 0.05$ were considered significant.

3. Results

3.1. Oxidative stress activates mitophagy but inhibits mitochondrial biogenesis, reduces mitochondrial mass, and impairs mitochondrial function in the HEI-OC1 cells

It is well documented that oxidative damage is a major cause leading to age-related cochlear hair cell loss and hearing loss (Yamasoba et al., 2013). Therefore, to explore the effect of oxidative stress on mitophagy and mitochondrial biogenesis in cochlear hair cells, we first conducted in vitro oxidative stress tests using H_2O_2 in the HEI-OC1 cells. H_2O_2 treatment significantly increased the levels of PINK1 and Parkin, and this increase presented in a time-dependant manner (Fig. 1A, D, and E). Because PINK1/Parkin signaling is the critical pathway in mitophagy induction, our results demonstrated that mitophagy was activated under oxidative stress. In addition, mitophagy induced by exposure to H_2O_2 was also evidenced by translocation of LC3 onto mitochondria (Fig. 1M). However, although the level of LC3-II was increased after the treatment of H_2O_2, which identifies autophagosomes and is an indicator of ongoing autophagy, the simultaneous presence of unchanged levels of p62 suggested a block in autophagosome degradation (Fig. 1A). In respect to mitochondrial biogenesis, PGC-1α and TFAM, 2 mitochondrial biogenesis-related genes, were decreased in response to H_2O_2 exposure (Fig. 1A–C). In addition, H_2O_2 exposure reduced the levels of the mitochondrial markers TOMM20 and COX4 (Fig. 1A, F, and G), indicating that mitochondrial content was decreased under oxidative stress. We also checked mitochondrial function by analyzing ATP production, ROS production, antioxidant enzyme level, and mitochondrial membrane potential. ATP levels were significantly reduced after the treatment of H_2O (Fig. 1H). The level of 4HNE, a marker for lipid peroxidation, was significantly increased in response to H_2O_2 exposure, whereas the expression of SOD1, a cytosolic antioxidant enzyme, was decreased (Fig. 1I–K). Compared with the control (Fig. 1L), flow cytometry analysis revealed a depolarization of the mitochondrial membrane in the HEI-OC1 cells treated with H_2O_2. These data suggest oxidative stress impaired mitochondrial function in the HEI-OC1 cells.

3.2. Modulation of miR-34a/SIRT1 signaling enhances mitophagy, mitochondrial biogenesis, and protects the HEI-OC1 cells against oxidative stress

Recent research has revealed that ursodeoxycholic acid (UDCA) targeted the miR-34a/SIRT1 signaling in the rat liver and primary rat hepatocytes and exerts significant antiapoptosis effects (Castro et al., 2013). Our previous study also showed that UDCA decreased miR-34a expression in the HEI-OC1 cells (Pang et al., 2017). Here, we revealed that miR-34a expression was increased during oxidative stress in a time-dependent manner, whereas SIRT1 expression was changed conversely (Fig. 2A and B). Then we confirmed that UDCA suppressed miR-34a expression and increased SIRT1 expression under both normal condition and

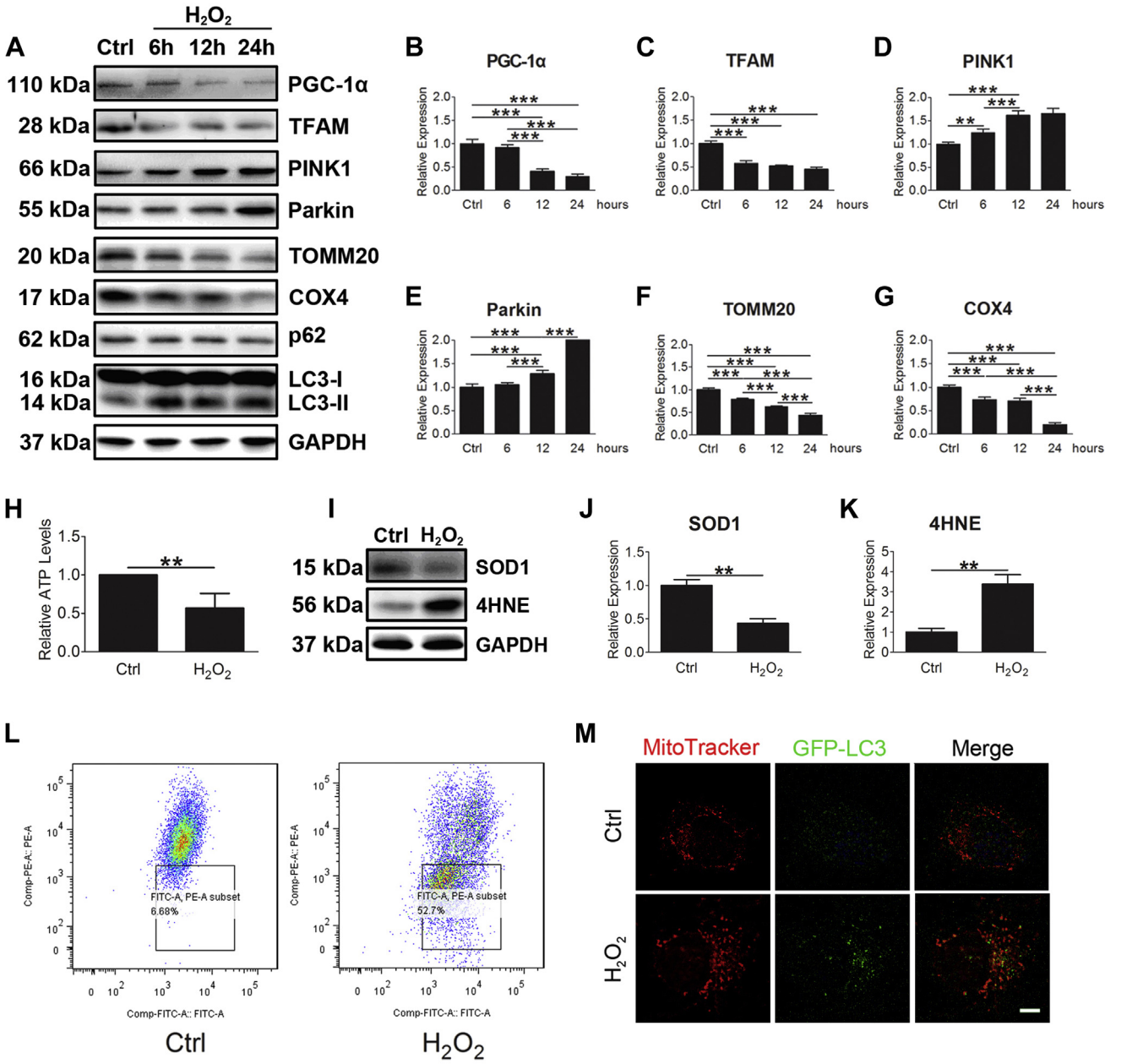

Fig. 1. Oxidative stress activates mitophagy, but inhibits mitochondrial biogenesis, reduces mitochondrial mass, and impairs mitochondrial function in the HEI-OC1 cells. (A–G) Western blotting and densitometry from controls and H_2O_2-exposed HEI-OC1 cells at various time points. Data are presented as means ± SD. n = 4 in each group. (H) ATP levels from controls and H_2O_2-exposed HEI-OC1 cells. n = 4 in each group. (I–K) Western blotting and densitometry from controls and H_2O_2-exposed HEI-OC1 cells. Data are presented as means ± SD. n = 3 in each group. (L) Mitochondrial membrane potential measurement from controls and H_2O_2-exposed HEI-OC1 cells. n = 3 in each group. (M) Translocation of LC3 onto mitochondria in H_2O_2-exposed HEI-OC1 cells. n = 3 in each group. ** $p < 0.01$, *** $p < 0.001$. Scale bar: 5 μm.

oxidative stress (Fig. 2C–E and I). Intriguingly, UDCA enhanced H_2O_2-induced elevation of mitophagy, evidenced by further increase of PINK1 (Fig. 2E, G, and J). To monitor mitophagy in the HEI-OC1 cells, mitochondria were visualized with fluorescent MitoTracker, and lysosomes were visualized based on the expression of the lysosomal marker LAMP1. UDCA increased the overlay between mitochondria and lysosomes in H_2O_2-treated cells compared with that did not receive UDCA treatment (Fig. 2K). Meanwhile, UDCA improved the decreased level of PGC-1α in the HEI-OC1 cells treated with H_2O_2, which implies partial recovery of mitochondrial biogenesis achieved by UDCA treatment (Fig. 2E and F). Accordingly, UDCA increased TOMM20 expression, demonstrating improvement in mitochondrial mass (Fig. 2E and H). Next, we investigated the protective role of modulation of miR-34a/SIRT1 signaling against oxidative stress in the HEI-OC1 cells. Treatment with H_2O_2 reduced cell viability in a dose-dependent manner. As predicted, UDCA-treated cells showed increased cell viability at multiple concentrations of H_2O_2 compared with control cells (Fig. 2L). Cells treated with SRT1720, a SIRT1 activator, also displayed increased cell viability in comparison with control cells (Fig. 2M). In addition, another SIRT1 activator resveratrol also reduced ROS level induced by H_2O_2 exposure (Supplementary Fig. 1A and B). These results demonstrate that modulation of miR-34a/SIRT1 signaling protects cochlear hair cells against oxidative

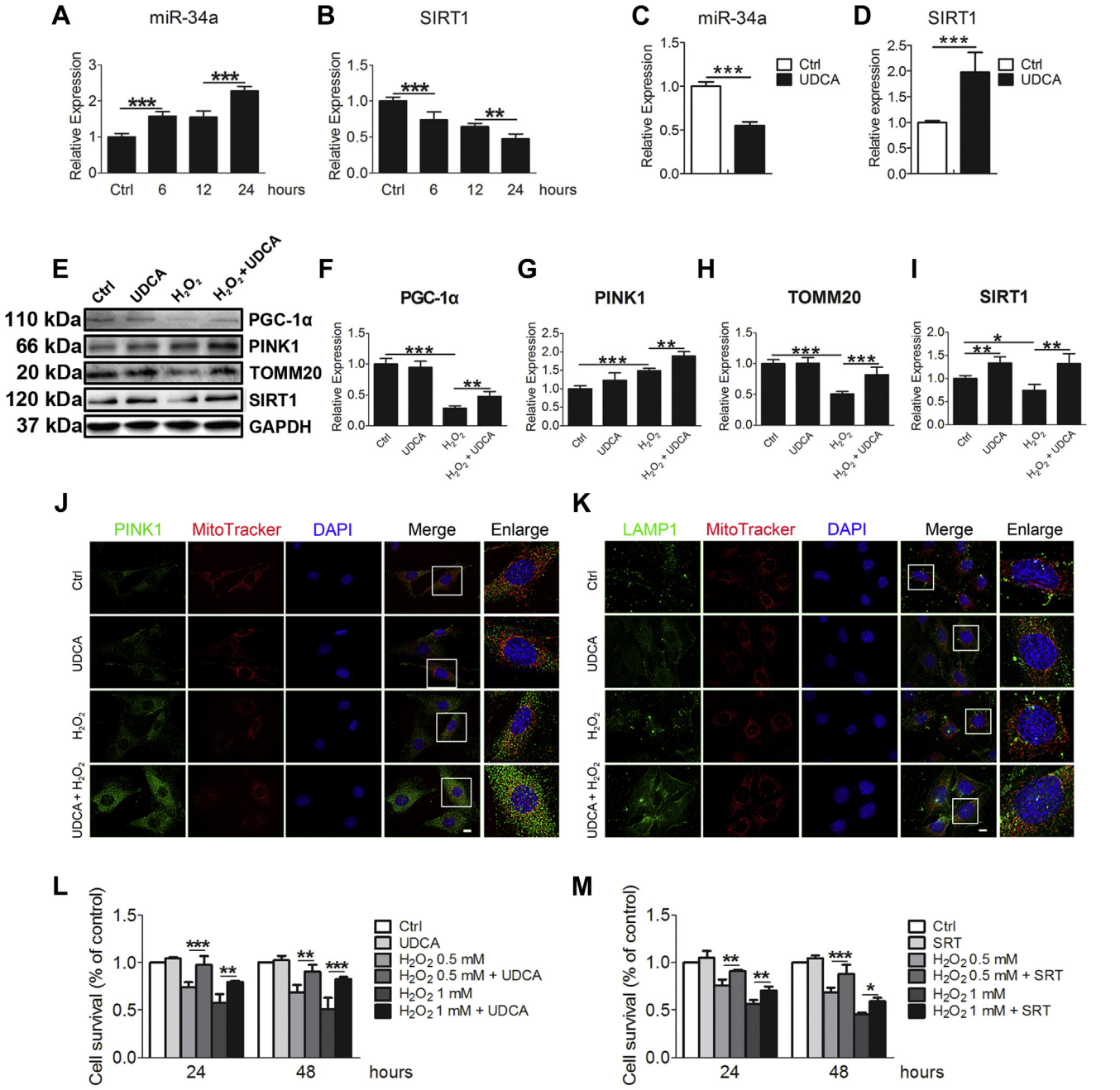

Fig. 2. Inhibition of miR-34a/SIRT1 signaling enhances mitophagy, mitochondrial biogenesis, and protects the HEI-OC1 cells against oxidative stress. (A and B) Expression of miR-34a and SIRT1 mRNA from controls and H_2O_2-exposed HEI-OC1 cells at various time points. Data are presented as means ± SD. n = 4 in each group. (C and D) Expression of miR-34a and SIRT1 mRNA from controls and HEI-OC1 cells treated with UDCA. Data are presented as means ± SD. n = 4 in each group. (E–I) Western blotting and densitometry from controls and H_2O_2-exposed HEI-OC1 cells with or without UDCA treatment. Data are presented as means ± SD. n = 4 in each group. (J) Immunocytochemistry for PINK1 from controls and H_2O_2-exposed HEI-OC1 cells with or without UDCA treatment. n = 3 in each group. (K) Immunocytochemistry for LAMP1 from controls and H_2O_2-exposed HEI-OC1 cells with or without UDCA treatment. n = 3 in each group. (L and M) The MTS assay from controls and H_2O_2-exposed HEI-OC1 cells with or without UDCA or SRT1720 treatment. Data are presented as means ± SD. n = 3 in each group. * $p < 0.05$, ** $p < 0.01$, *** $p < 0.001$. Scale bar: 5 μm.

stress. To clarify the involvement of activated mitophagy in miR-34a/SIRT1 signaling–mediated protection, we blocked mitophagy by silencing Parkin, a gene that is essential for mitophagy induction, with small interfering RNA (siParkin) in the HEI-OC1 cells. Western blot analysis showed a nearly 50% reduction of Parkin expression in siRNA-transfected cells (Supplementary Fig. 2A and B). Knockdown of Parkin before UDCA treatment abolished its protective effects as reflected by the reversed cell viability (Supplementary Fig. 2C). Moreover, inhibition of mitophagy by silencing Drp1, which is required for mitochondrial fission, exacerbated oxidative damage to the HEI-OC1 cells (Supplementary Fig. 2G). Similarly, inhibition of mitochondrial biogenesis by silencing PGC-1α also reduced the protective effects of UDCA (Supplementary Fig. 2D–F). These data offer support for the hypothesis that mitophagy and mitochondrial biogenesis are involved in miR-34a/SIRT1 signaling–mediated protection against oxidative stress.

3.3. Aging causes increased mitophagy and mitochondrial biogenesis in the cochlea of C57BL/6 mice

It is unclear that whether mitochondrial homeostasis is maintained in the cochlea during aging. Therefore, we checked the level of mitophagy and mitochondrial biogenesis in young and old C57BL/6 mice. Western blotting analysis showed PINK1 and PGC-1α expressions were both elevated in the cochlea of old mice compared with those in young mice (Fig. 3A–C). These data suggest that increased mitophagy and mitochondrial biogenesis were induced in the cochlea of C57BL/6 mice with aging. Increased levels of mitophagy and mitochondrial biogenesis were further confirmed

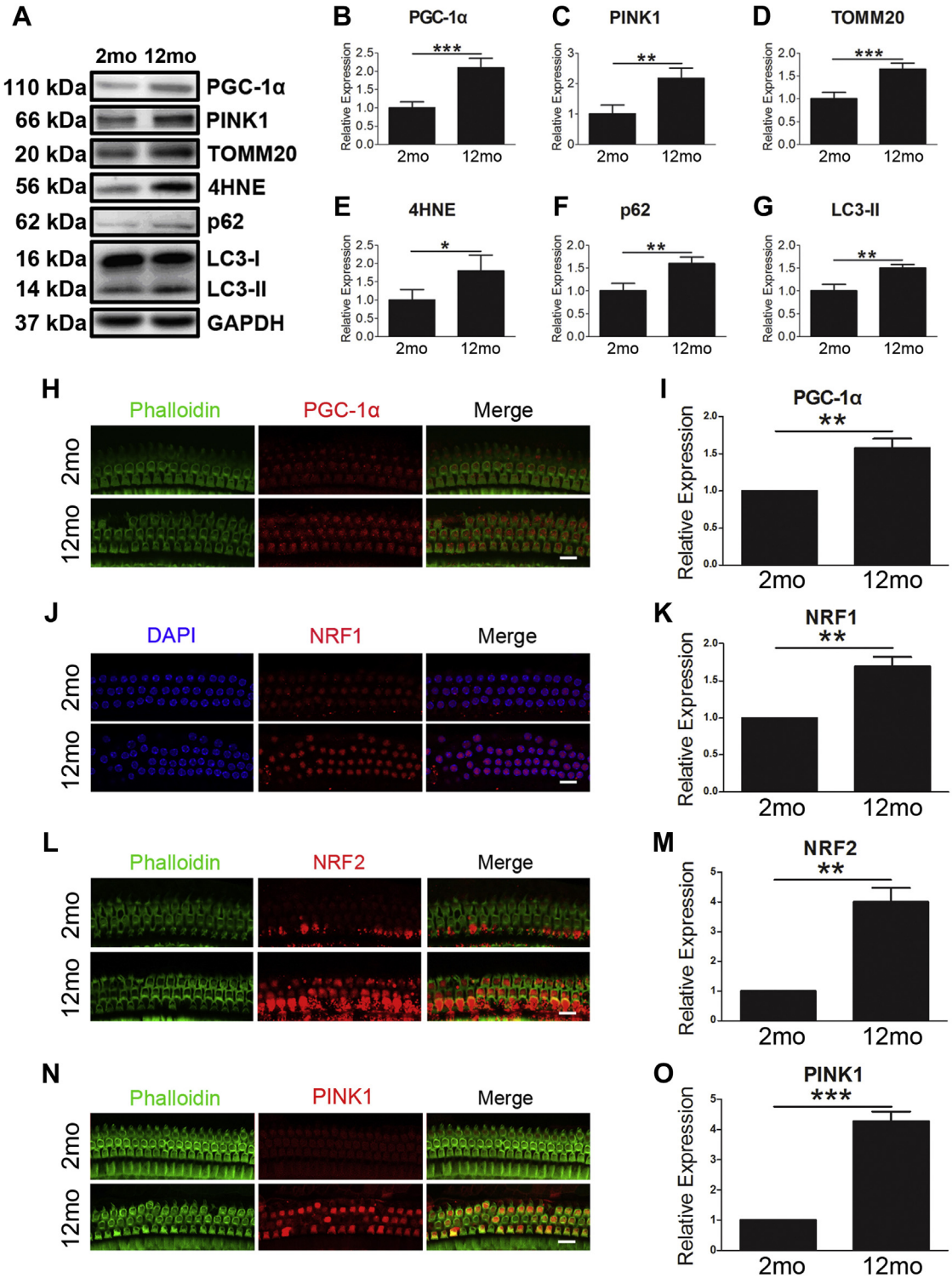

Fig. 3. Aging causes increased mitophagy and mitochondrial biogenesis in the cochlea of C57BL/6 mice. (A–G) Western blotting and densitometry from the cochlea of C57BL/6 mice at 2 and 12 months of age. Data are presented as means ± SD. n = 8 in each group. (H–O) Immunolabeling and quantification for PGC-1α, NRF1, NRF2, and PINK1 in outer hair cells of surface preparations from C57BL/6 mice at 2 and 12 months of age. Data are presented as means ± SD. n = 4 in each group. * $p < 0.05$, ** $p < 0.01$, *** $p < 0.001$. Scale bar: 10 μm.

by immunocytochemistry for cochlear surface preparations. Immunoreactivity for PGC-1α, NRF1, NRF2, and PINK1 were stronger in the OHCs of old C57BL/6 mice in comparison with that in young mice (Fig. 3H, J, L, and N). Quantification of immunolabeling for PGC-1α and NRF1 in OHCs around the 16–22 kHz region confirmed a significant increase by about 50% in old mice compared with young mice, while aging led to a 4-fold increase in PINK1 and NRF2 expression (Fig. 3I, K, M, and O). Although mitophagy was activated with aging, a blocked autophagic flux was noted, evidenced by simultaneously increased level of LC3-II and p62 (Fig. 3A, F, and G). In addition, the upregulation of TOMM20 in the old mice suggests an accumulation in mitochondrial mass with aging (Fig. 3A and D). Moreover, 4HNE expression was increased in old mice, which implies an elevated level of oxidative stress (Fig. 3A and E).

3.4. Activation of SIRT1 by resveratrol delays AHL, protects cochlear hair cells, and SGNs in C57BL/6 mice

Our previous studies have showed that miR-34a/SIRT1 is activated during aging in the cochlea of C57BL/6 mice (Pang et al., 2017; Xiong et al., 2015). Because modulation of miR-34a/SIRT1 signaling improved the balance between mitophagy and mitochondrial biogenesis and protected cells against oxidative stress in the HEI-OC1 cells, we next investigate whether this signaling exerts similar protective effects against age-related cochlear hair cell loss and AHL. C57BL/6 mice at 2 months were subjected to dietary supplementation with 2 different doses of resveratrol (7.5 or 300 mg/kg/d) added to the chow for a period of 10 months. High dose of resveratrol at 300 mg/kg/d significantly reduced age-related auditory threshold shifts at 8, 16, and 32 kHz, whereas relatively low dose of resveratrol at 7.5 mg/kg/d attenuated ABR threshold shifts at 8 and 16 kHz (Fig. 4A). Treatment with resveratrol at 2 doses also significantly reduced age-related OHC loss from 1.5 to 3.5 mm from apex along the cochlear epithelium (Fig. 4B and Supplementary Fig. 3A). Although age-related IHC loss was only observed in the basal turn of the cochlea and was not affected by resveratrol treatment, age-related loss of IHC synaptic ribbons was attenuated by resveratrol treatment (Supplementary Fig. 3B). Intriguingly, C57BL/6 mice treated with rapamycin, a well-known autophagy activator, displayed a less loss of OHCs and IHC synaptic ribbons during aging as well (Supplementary Fig. 3A and B). Because age-related loss of SGNs and atrophy stria vascularis are also major pathological characters of AHL, we then performed histological analysis on cochlear tissue sections from mice with different treatment. Resveratrol treatment remarkably attenuated the degeneration of SGNs and reduced stria vascularis thickness at the middle cochlear turn in old C57BL/6 mice compared with those fed standard chow (Fig. 4C–F). Collectively, these results demonstrate that resveratrol protects cochlear OHCs, SGNs, and stria vascularis and delays AHL in C57BL/6 mice.

3.5. Activation of SIRT1 by resveratrol improves the balance between mitophagy and mitochondrial biogenesis in the cochlea of C57BL/6 mice with aging

To determine the role of mitochondrial homeostasis in miR-34a/SIRT1 signaling–conferred protection, we then examined the levels of mitophagy and mitochondrial biogenesis in mice with different treatment. First, we confirmed that mitophagy was activated in the aging cochlea based on the findings that PINK1 and Parkin expression were both increased. In consistent with findings in the HEI-OC1 cells, modulation of miR-34a/SIRT1 by resveratrol further increased the level of PINK1 and Parkin in old mice compared with age-matched mice, indicating mitophagy was enhanced by miR-34a/SIRT1 signaling (Fig. 5A, F, and G). Meanwhile, mice with resveratrol treatment showed lower levels of LC3-II and p62 in comparison with control mice, which means a partial recovery in autophagic flux in old mice (Fig. 5A, L, and M). Similarly, treatment of resveratrol reversed the elevated levels of PGC-1α, NRF1, NRF2, and TFAM with aging, suggesting the level of mitochondrial biogenesis was suppressed by modulation of miR-34a/SIRT1 signaling (Fig. 5B–E). The effect of resveratrol on the expression pattern of PINK1 and PGC-1α during aging was further confirmed by immunohistochemistry of cochlear surface preparations (Fig. 5N–Q). Enhanced mitophagy and reduced mitochondrial biogenesis induced by resveratrol undoubtedly decreased mitochondrial mass in the aging cochlea, evidenced by decreased levels of TOMM20 and COX4 (Fig. 5A, H, I and Supplementary Fig. 4B) and further confirmed by direct measurement of the amount of mitochondrial DNA from cochlear tissues (Supplementary Fig. 4C). Consequently, the decreased level of 4HNE and increased level of SOD1 in mice treated with resveratrol demonstrate that activation of miR-34a/SIRT1 signaling improved mitochondrial function in old C57BL/6 mice (Fig. 5A, J, K and Supplementary Fig. 4A). Similarly, C57BL/6 mice treated with rapamycin showed the similar effects on mitophagy, mitochondrial biogenesis, and mitochondrial function as resveratrol (Fig. 5A–Q; Supplementary Fig. 4A–C). Taken together, these data suggest that modulation of miR-34a/SIRT1 by resveratrol improved the balance between mitophagy and mitochondrial biogenesis in the cochlea with aging.

3.6. Overexpression of SIRT1 or knockdown of miR-34a protects cochlear cells and delays AHL in C57BL/6 mice

To further determine the protective role of miR-34a/SIRT1 signaling in AHL, SIRT1 Tg mice and miR-34a$^{+/-}$ mice were used in the present study. The genotypes of SIRT1 Tg mice and miR-34a$^{+/-}$ mice were verified by polymerase chain reaction screening (Fig. 6A and Supplementary Fig. 5A). SIRT1 Tg mice displayed a 3-fold increase in SIRT1 expression compared with wild-type mice (Fig. 6B). As predicted, SIRT1 Tg mice at 12 months of age showed a significant reduction of age-related auditory threshold shifts at 8, 16, and 32 kHz relative to wild-type mice (Fig. 6C). Moreover, SIRT1 Tg mice exhibited reduced age-related OHC loss at cochlear spiral from 1.5 to 4.5 mm from apex (Fig. 6D). Similarly, overexpression of SIRT1 did not affect age-related IHC loss (Fig. 6D). Comparably, miR-34a$^{+/-}$ mice exhibited a decrease by 50% in miR-34a expression compared with wild-type mice (Supplementary Fig. 5B). Interestingly, miR-34a$^{+/-}$ mice at 14 months of age showed a reduced age-related auditory threshold shifts at 16 kHz compared with age-matched wild-type mice (Supplementary Fig. 5C). Threshold shifts at 8 kHz in miR-34a$^{+/-}$ mice showed a tendency to decrease compared with wild-type mice but did not reach statistical significance. Threshold shifts at 32 kHz showed no difference between miR-34a$^{+/-}$ mice and wild-type mice. Accordingly, miR-34a$^{+/-}$ mice also exhibited reduced age-related OHC loss at cochlear spiral from 2 to 3 mm from apex (Supplementary Fig. 5D). There were no differences in IHC loss between the 2 genotypes of mice (Supplementary Fig. 5D). Overall, these findings further support a protective role of modulation of miR-34a/SIRT1 signaling in age-related cochlear hair cell loss and AHL.

4. Discussion

Mitochondrial function determines several molecular signaling which modulates cellular metabolism, cell survival, and health span. Impairment of mitochondrial function has been involved in a variety of pathological conditions and aging. Mitophagy and mitochondrial biogenesis, 2 opposing cellular pathways, coordinately regulate mitochondrial turnover and homeostasis to maintain

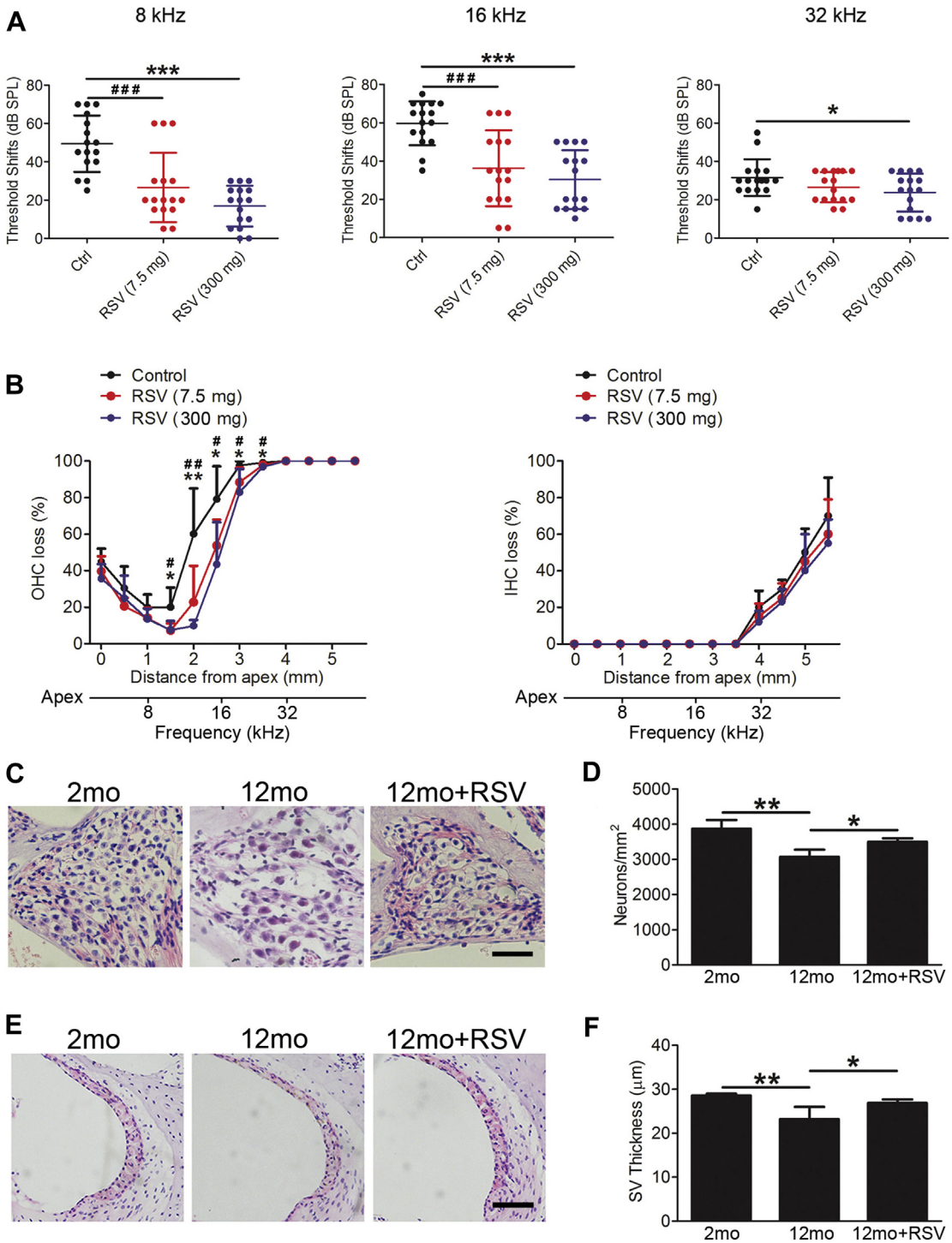

Fig. 4. Resveratrol delays AHL and protects cochlear hair cells and spiral ganglion neurons in C57BL/6 mice. (A) ABR threshold shifts measured in C57BL/6 mice treated with resveratrol and controls. Data are presented as individual points and means ± SD. (B) Hair cell counts in C57BL/6 mice treated with resveratrol and controls. Data are presented as means ± SD. n = 5 in each group. (C and D) Spiral ganglion neuron counts at the middle cochlear turn in C57BL/6 mice treated with resveratrol and controls. Data are presented as means ± SD. n = 3 in each group. (E and F) Stria vascularis thickness measurements at the middle cochlear turn in C57BL/6 mice treated with resveratrol and controls. Data are presented as means ± SD. n = 3 in each group. * $p < 0.05$, ** $p < 0.01$, *** $p < 0.001$ (Ctrl vs. RSV at 300 mg). # $p < 0.05$, ## $p < 0.01$, ### $p < 0.001$ (Ctrl vs. RSV at 7.5 mg). Scale bar: 100 μm. Abbreviations: AHL, Age-related hearing loss; ABR, auditory brainstem response; IHC, inner hair cell; OHC, outer hair cell; RSV, resveratrol.

cellular energy metabolism and enable cell to survive in response to multiple types of stress and insults (Palikaras et al., 2015a; Palikaras and Tavernarakis, 2014). Because aging is suggested to be a leading factor for reductions in mitochondrial capacity (Bua et al., 2006; Kim et al., 2017), the investigation into mitochondrial quality control through mitophagy and mitochondrial biogenesis is fundamentally essential to advance our understanding of the pathogenesis of age-related cochlear hair cell loss and AHL.

Consistent with previous studies (Artal-Sanz and Tavernarakis, 2009; Kaeberlein, 2010), we firstly observed mitochondrial accumulation and decreased mitochondrial function in the cochlea of C57BL/6 mice during aging, which are the typical phenotypes of

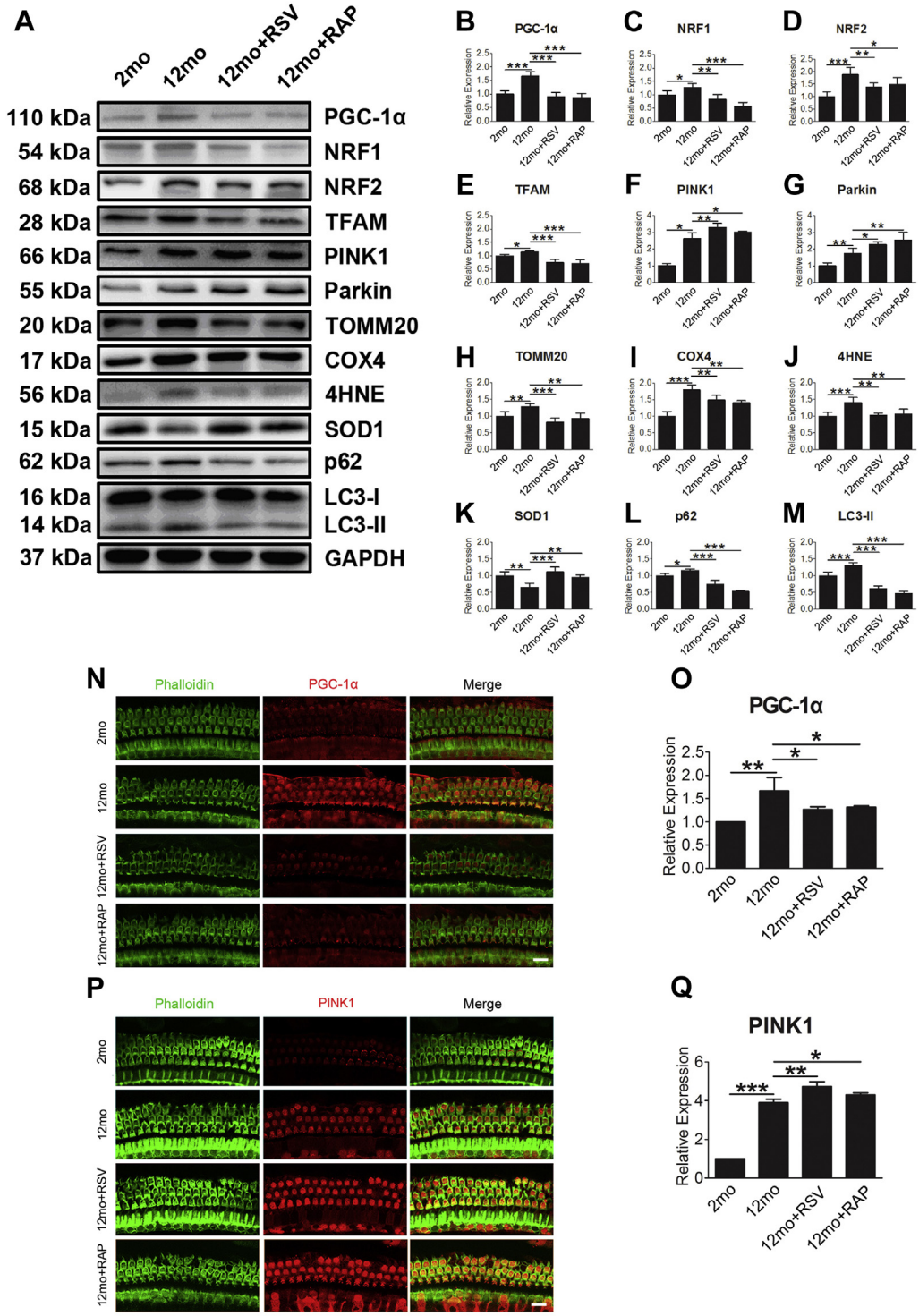

Fig. 5. Resveratrol and rapamycin improves the balance between mitophagy and mitochondrial biogenesis in the cochlea of C57BL/6 mice with aging. (A–M) Western blotting and densitometry from the cochlea of C57BL/6 mice treated with resveratrol or rapamycin and controls. Data are presented as means ± SD. n = 8 in each group. (N–Q) Immunolabeling and quantification for PGC-1α and PINK1 in outer hair cells of surface preparations from the cochlea of C57BL/6 mice treated with resveratrol or rapamycin and controls. Data are presented as means ± SD. n = 4 in each group. * $p < 0.05$, ** $p < 0.01$, *** $p < 0.001$. Scale bar: 10 μm. Abbreviations: RSV, resveratrol; RAP, rapamycin.

aging. We then examined whether mitophagy and mitochondrial biogenesis are involved in age-related mitochondrial dysfunction. Strikingly, although the progressive decline of autophagy activity is regarded as a major hallmark of the aging process and our present findings indicate autophagic flux is also blocked (Lionaki et al., 2013; Schiavi and Ventura, 2014), mitophagy is selectively activated in the cochlea of aging C57BL/6 mice, evident by increased level of PINK1 and Parkin. PINK1/Parkin signaling is critical to the maintenance of mitochondrial integrity and function via mitophagy (Geisler et al., 2010a,b). On membrane depolarization, PINK1 is stabilized and activated by damaged mitochondria, resulting in the recruitment of Parkin from the cytosol to the mitochondria (Nguyen et al., 2016) and initiates mitophagy subsequently. Our findings are consistent with a recent study showing that Parkin-mediated

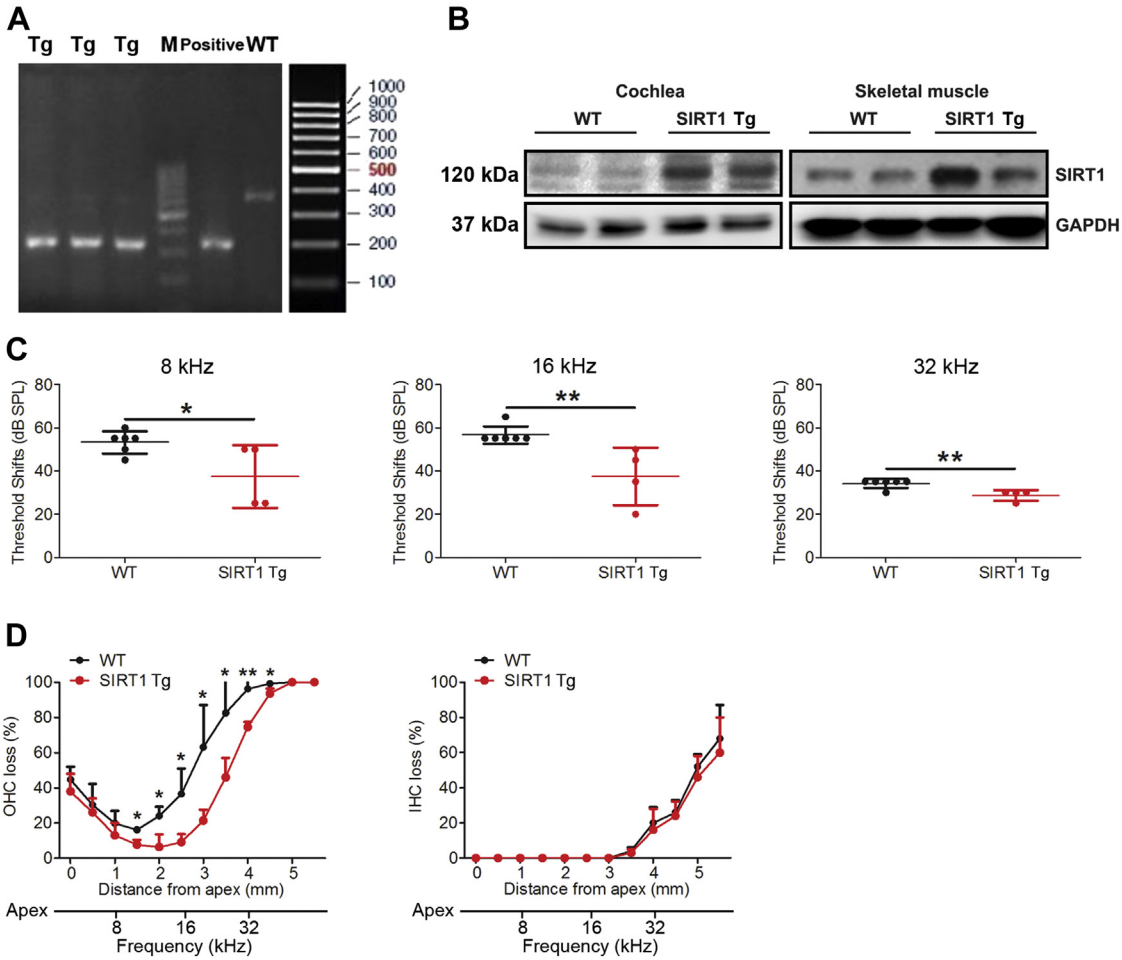

Fig. 6. Overexpression of SIRT1 protects cochlear cells and delays AHL in C57BL/6 mice. (A) Genotyping for SIRT1 Tg mice. (B) Western blotting for SIRT1 from SIRT1 Tg mice and wild types. (C) ABR threshold shifts measured in SIRT1 Tg mice and wild types. Data are presented as individual points and means ± SD. (D) Hair cell counts in SIRT1 Tg mice and wild types. Data are presented as means ± SD. n = 4 in each group. * $p < 0.05$, ** $p < 0.01$. Abbreviations: AHL, age-related hearing loss; IHC, inner hair cell; M, marker; OHC, outer hair cell; Tg, transgenic mice; WT, wild type.

mitophagy is enhanced in the brain from patients with Alzheimer's disease, the most common neurodegenerative disease, which indicates that aberrant accumulation of dysfunctional mitochondria in Alzheimer's disease–affected neurons is probably attributed to inadequate mitophagy capacity in removal of increased damaged mitochondria (Ye et al., 2015). On the other hand, although reduced mitochondrial protein content are common findings in aging (Kim et al., 2017; Zhu et al., 2013), our data reveal mitochondrial biogenesis–related proteins such as PGC-1α, NRF1, NRF2, and TFAM are upregulated in the cochlea of aging C57BL/6 mice, suggesting mitochondrial biogenesis is activated in the cochlea with aging. PGC-1α is characterized as the master regulator of mitochondrial biogenesis and function (Andres et al., 2015). PGC-1α regulates the expression of NRF1 and NRF2, which in turn control the expression of TFAM. TFAM modulates the expression of several mitochondrial genes, playing a key role in mitochondrial biogenesis. Our results are consistent with previous study that increase in the expression PGC-1α, NRF1, and TFAM is observed in the auditory cortex of D-galactose–induced mimetic aging rats with aging (Zhong et al., 2012). Taken together, our present study provides new insights into mitophagy and mitochondrial biogenesis in cochlea aging: during aging, dysfunctional mitochondria are accumulated and mitochondrial function is decreased progressively. Although age-related mitochondrial stress is sufficient to induce mitophagy, such mitophagy capacity is still inadequate to remove increased numbers of damaged mitochondria. Meanwhile, mitochondrial biogenesis is activated as a compensatory response to produce newly healthy mitochondria and improve mitochondrial function, although it seems that such compensation is insufficient. Moreover, compensatory increase in mitochondrial biogenesis may also promote the production of mutated mtDNA, leading to further overall mitochondrial dysfunction (Kim et al., 2017).

We next explored whether coordinated regulation of mitophagy and mitochondrial biogenesis improves mitochondrial function and reduced mitochondrial mass in the aging cochlea. Our previous studies have confirmed that miR-34a/SIRT1 signaling is involved in the regulation of autophagic flux in the cochlea and correlated with cochlear degeneration and AHL in C57BL/6 mice (Pang et al., 2017; Xiong et al., 2014, 2015). Intriguingly, SIRT1, an NAD-dependent lysine deacetylase, not only activates autophagy by deacetylating multiple autophagy-related proteins, such as Atg7, Atg5, and Atg8 (Morita et al., 2013) but also selectively stimulates mitophagy through regulation of UCP2 (Fang et al., 2014). In addition, SIRT1 is well known to regulate mitochondrial biogenesis via activation of PGC-1α as well (Tang, 2016). Here, we found long-term administration of SIRT1 activator resveratrol further enhances mitophagy, attenuates elevated mitochondrial biogenesis, and improves mitochondrial function in the aging cochlea. The rescue of

mitochondrial function appears to be attributed to removal of damaged or superfluous mitochondria by enhanced mitophagy activity. Therefore, reduced mitochondrial stress does not trigger excessive mitochondrial biogenesis any longer. Moreover, resveratrol treatment reduces age-related cochlear cell loss, stria vascularis atrophy, and delays AHL in C57BL/6 mice. In addition, overexpression of SIRT1 recapitulates the effect of resveratrol on auditory function in aging C57BL/6 mice. miR-34a deficiency also shows a weaker protective role against age-related cochlear hair cell loss and AHL in C57BL/6 mice. These results show for the first time that modulation of miR-34a/SIRT1 signaling rescues mitochondrial function, attenuates age-related cochlear hair cell loss, and delays AHL at least partially by coordinated regulation of mitophagy and mitochondrial biogenesis.

Oxidative damage has been proposed to be a major cause leading to age-related cochlear hair cell loss and hearing loss (Yamasoba et al., 2013). Therefore, we also investigated mitophagy and mitochondrial biogenesis in vitro oxidative stress tests using H_2O_2 in the HEI-OC1 cells. Our findings show oxidative stress induced by H_2O_2 activates mitophagy, but suppresses mitochondrial biogenesis, therefore leading to mitochondrial mass loss and mitochondrial dysfunction, which is consistent with the previous studies that showing H_2O_2 promotes mitophagy and inhibits mitochondrial biogenesis in multiple types of cells (Choi et al., 2017; Ren et al., 2017; Yans et al., 2015). Meanwhile, miR-34a/SIRT1 signaling is activated as well under oxidative stress. Treatment with miR-34a inhibitor UDCA further enhances mitophagy and promotes mitochondrial biogenesis, rescues mitochondrial mass, and attenuates cell death subsequently. Intriguingly, the protective effect of UDCA is abolished by inhibition of PINK1 or PGC-1α. Similarly, treatment with SIRT1 activator resveratrol alleviates mitochondrial ROS production and protects the HEI-OC1 cells from oxidative stress. These findings confirm that oxidative stress breaks the balance between mitophagy and mitochondrial biogenesis, contributing to the HEI-OC1 cell death. Modulation of miR-34a/SIRT1 protects the HEI-OC1 cells against oxidative stress by coordinated regulation of mitophagy and mitochondrial biogenesis.

The present study has several limitations. First, although oxidative stress is a major cause for age-related cochlear hair cell loss and AHL, other risk factors such as impaired homeostasis of cochlear blood supply and genetic predisposition also contribute to the pathogenesis of AHL (Yamasoba et al., 2013). These may explain the large variations of the onset and extent of AHL among humans. Therefore, in the present study, oxidative stress induced by H_2O_2 activates mitophagy and inhibits mitochondrial biogenesis in the HEI-OC1 cells, whereas mitophagy and mitochondrial biogenesis are both activated in the cochlea of C57BL/6 mice during aging. These discrepancies may be due to multiple causes for cochlea aging other than oxidative stress. Establishing a senescence cochlear hair cell model to elucidate the detailed mechanisms underlying the relationship between mitochondrial homeostasis and AHL is required in the further study. Second, although modulation of miR-34a/SIRT1 signaling is suggested to improve the balance between mitophagy and mitochondrial biogenesis and protects cochlear hair cells against oxidative stress and aging in the present study, the full signaling pathway involved in this process has not been elucidated. For instance, SIRT1 and AMPK are well known to promote each other's function reciprocally and play an important role during aging process (Lapierre et al., 2015; Satoh et al., 2017). Intriguingly, SIRT1/AMPK signaling is recently implicated in the fine-tuning of coordination of mitophagy and mitochondrial biogenesis (Palikaras et al., 2015a; Zhu et al., 2013). It would be of interest to explore the modulation of mitochondrial turnover by miR-34a/SIRT1/AMPK signaling in cochlear pathology in a further investigation.

5. Conclusions

In summary, our present study demonstrates that imbalance of mitophagy and mitochondrial biogenesis is presented in the cochlear hair cells during aging or under oxidative stress, which contributes to mitochondrial dysfunction and cell damage. Modulation of miR-34a/SIRT1 signaling improves mitochondrial function, protects cochlear hair cell, and delays AHL through coordinated regulation of mitophagy and mitochondrial biogenesis. Our findings may provide the basis for novel therapeutic strategies against cochlear degeneration and AHL through simultaneously targeting mitophagy and mitochondrial biogenesis.

Disclosure

The authors declare that they have no competing interests.

Acknowledgements

This work was supported by the National Natural Science Foundation of China (81570916, 81771018 and 81873699) and Yat-Sen Scholarship for Young Scientist.

Appendix A. Supplementary data

Supplementary data associated with this article can be found, in the online version, at https://doi.org/10.1016/j.neurobiolaging.2019.03.013.

References

Andres, A.M., Stotland, A., Queliconi, B.B., Gottlieb, R.A., 2015. A time to reap, a time to sow: mitophagy and biogenesis in cardiac pathophysiology. J. Mol. Cell. Cardiol. 78, 62–72.
Artal-Sanz, M., Tavernarakis, N., 2009. Prohibitin couples diapause signalling to mitochondrial metabolism during ageing in C. elegans. Nature 461, 793–797.
Bartel, D.P., 2018. Metazoan MicroRNAs. Cell 173, 20–51.
Bielefeld, E.C., Tanaka, C., Chen, G.D., Henderson, D., 2010. Age-related hearing loss: is it a preventable condition? Hear. Res. 264, 98–107.
Boon, R.A., Iekushi, K., Lechner, S., Seeger, T., Fischer, A., Heydt, S., Kaluza, D., Treguer, K., Carmona, G., Bonauer, A., Horrevoets, A.J., Didier, N., Girmatsion, Z., Biliczki, P., Ehrlich, J.R., Katus, H.A., Muller, O.J., Potente, M., Zeiher, A.M., Hermeking, H., Dimmeler, S., 2013. MicroRNA-34a regulates cardiac ageing and function. Nature 495, 107–110.
Bua, E., Johnson, J., Herbst, A., Delong, B., McKenzie, D., Salamat, S., Aiken, J.M., 2006. Mitochondrial DNA-deletion mutations accumulate intracellularly to detrimental levels in aged human skeletal muscle fibers. Am. J. Hum. Genet. 79, 469–480.
Castro, R.E., Ferreira, D.M., Afonso, M.B., Borralho, P.M., Machado, M.V., Cortez-Pinto, H., Rodrigues, C.M., 2013. miR-34a/SIRT1/p53 is suppressed by ursodeoxycholic acid in the rat liver and activated by disease severity in human non-alcoholic fatty liver disease. J. Hepatol. 58, 119–125.
Choi, H.I., Kim, H.J., Park, J.S., Kim, I.J., Bae, E.H., Ma, S.K., Kim, S.W., 2017. PGC-1alpha attenuates hydrogen peroxide-induced apoptotic cell death by upregulating Nrf-2 via GSK3beta inactivation mediated by activated p38 in HK-2 Cells. Sci. Rep. 7, 4319.
Di Sante, G., Pestell, T.G., Casimiro, M.C., Bisetto, S., Powell, M.J., Lisanti, M.P., Cordon-Cardo, C., Castillo-Martin, M., Bonal, D.M., Debattisti, V., Chen, K., Wang, L., He, X., McBurney, M.W., Pestell, R.G., 2015. Loss of Sirt1 promotes prostatic intraepithelial neoplasia, reduces mitophagy, and delays PARK2 translocation to mitochondria. Am. J. Pathol. 185, 266–279.
Fang, E.F., Scheibye-Knudsen, M., Brace, L.E., Kassahun, H., SenGupta, T., Nilsen, H., Mitchell, J.R., Croteau, D.L., Bohr, V.A., 2014. Defective mitophagy in XPA via PARP-1 hyperactivation and NAD(+)/SIRT1 reduction. Cell 157, 882–896.
Gates, G.A., Mills, J.H., 2005. Presbycusis. Lancet 366, 1111–1120.
Geisler, S., Holmstrom, K.M., Skujat, D., Fiesel, F.C., Rothfuss, O.C., Kahle, P.J., Springer, W., 2010a. PINK1/Parkin-mediated mitophagy is dependent on VDAC1 and p62/SQSTM1. Nat. Cell Biol. 12, 119–131.
Geisler, S., Holmstrom, K.M., Treis, A., Skujat, D., Weber, S.S., Fiesel, F.C., Kahle, P.J., Springer, W., 2010b. The PINK1/Parkin-mediated mitophagy is compromised by PD-associated mutations. Autophagy 6, 871–878.
Guo, Y., Li, P., Gao, L., Zhang, J., Yang, Z., Bledsoe, G., Chang, E., Chao, L., Chao, J., 2017. Kallistatin reduces vascular senescence and aging by regulating microRNA-34a-SIRT1 pathway. Aging Cell 16, 837–846.

Herskovits, A.Z., Guarente, L., 2014. SIRT1 in neurodevelopment and brain senescence. Neuron 81, 471–483.
Homans, N.C., Metselaar, R.M., Dingemanse, J.G., van der Schroeff, M.P., Brocaar, M.P., Wieringa, M.H., Baatenburg de Jong, R.J., Hofman, A., Goedegebure, A., 2017. Prevalence of age-related hearing loss, including sex differences, in older adults in a large cohort study. Laryngoscope 127, 725–730.
Kaeberlein, M., 2010. Lessons on longevity from budding yeast. Nature 464, 513–519.
Kim, Y., Triolo, M., Hood, D.A., 2017. Impact of aging and exercise on mitochondrial quality control in skeletal muscle. Oxid. Med. Cell. Longev. 2017, 3165396.
Lapierre, L.R., Kumsta, C., Sandri, M., Ballabio, A., Hansen, M., 2015. Transcriptional and epigenetic regulation of autophagy in aging. Autophagy 11, 867–880.
Lionaki, E., Markaki, M., Tavernarakis, N., 2013. Autophagy and ageing: insights from invertebrate model organisms. Ageing Res. Rev. 12, 413–428.
Liu, N., Landreh, M., Cao, K., Abe, M., Hendriks, G.J., Kennerdell, J.R., Zhu, Y., Wang, L.S., Bonini, N.M., 2012. The microRNA miR-34 modulates ageing and neurodegeneration in Drosophila. Nature 482, 519–523.
Lopez-Otin, C., Blasco, M.A., Partridge, L., Serrano, M., Kroemer, G., 2013. The hallmarks of aging. Cell 153, 1194–1217.
Morita, M., Gravel, S.P., Chenard, V., Sikstrom, K., Zheng, L., Alain, T., Gandin, V., Avizonis, D., Arguello, M., Zakaria, C., McLaughlan, S., Nouet, Y., Pause, A., Pollak, M., Gottlieb, E., Larsson, O., St-Pierre, J., Topisirovic, I., Sonenberg, N., 2013. mTORC1 controls mitochondrial activity and biogenesis through 4E-BP-dependent translational regulation. Cell Metab. 18, 698–711.
Mouchiroud, L., Houtkooper, R.H., Moullan, N., Katsyuba, E., Ryu, D., Canto, C., Mottis, A., Jo, Y.S., Viswanathan, M., Schoonjans, K., Guarente, L., Auwerx, J., 2013. The NAD(+)/Sirtuin pathway modulates longevity through activation of mitochondrial UPR and FOXO signaling. Cell 154, 430–441.
Nguyen, T.N., Padman, B.S., Usher, J., Oorschot, V., Ramm, G., Lazarou, M., 2016. Atg8 family LC3/GABARAP proteins are crucial for autophagosome-lysosome fusion but not autophagosome formation during PINK1/Parkin mitophagy and starvation. J. Cell Biol. 215, 857–874.
Palikaras, K., Lionaki, E., Tavernarakis, N., 2015a. Balancing mitochondrial biogenesis and mitophagy to maintain energy metabolism homeostasis. Cell Death Differ. 22, 1399–1401.
Palikaras, K., Lionaki, E., Tavernarakis, N., 2015b. Coordination of mitophagy and mitochondrial biogenesis during ageing in C. elegans. Nature 521, 525–528.
Palikaras, K., Tavernarakis, N., 2014. Mitochondrial homeostasis: the interplay between mitophagy and mitochondrial biogenesis. Exp. Gerontol. 56, 182–188.
Pang, J., Xiong, H., Lin, P., Lai, L., Yang, H., Liu, Y., Huang, Q., Chen, S., Ye, Y., Sun, Y., Zheng, Y., 2017. Activation of miR-34a impairs autophagic flux and promotes cochlear cell death via repressing ATG9A: implications for age-related hearing loss. Cell Death Dis. 8, e3079.
Patel, M., Hu, B.H., 2012. MicroRNAs in inner ear biology and pathogenesis. Hear. Res. 287, 6–14.
Price, N.L., Gomes, A.P., Ling, A.J., Duarte, F.V., Martin-Montalvo, A., North, B.J., Agarwal, B., Ye, L., Ramadori, G., Teodoro, J.S., Hubbard, B.P., Varela, A.T., Davis, J.G., Varamini, B., Hafner, A., Moaddel, R., Rolo, A.P., Coppari, R., Palmeira, C.M., de Cabo, R., Baur, J.A., Sinclair, D.A., 2012. SIRT1 is required for AMPK activation and the beneficial effects of resveratrol on mitochondrial function. Cell Metab. 15, 675–690.
Ren, Y., Li, Y., Yan, J., Ma, M., Zhou, D., Xue, Z., Zhang, Z., Liu, H., Yang, H., Jia, L., Zhang, L., Zhang, Q., Mu, S., Zhang, R., Da, Y., 2017. Adiponectin modulates oxidative stress-induced mitophagy and protects C2C12 myoblasts against apoptosis. Sci. Rep. 7, 3209.
Satoh, A., Imai, S.I., Guarente, L., 2017. The brain, sirtuins, and ageing. Nat. Rev. Neurosci. 18, 362–374.
Schiavi, A., Ventura, N., 2014. The interplay between mitochondria and autophagy and its role in the aging process. Exp. Gerontol. 56, 147–153.
Tang, B.L., 2016. Sirt1 and the mitochondria. Mol. Cells 39, 87–95.
Wilson, B.S., Tucci, D.L., Merson, M.H., O'Donoghue, G.M., 2017. Global hearing health care: new findings and perspectives. Lancet 390, 2503–2515.
Xiong, H., Dai, M., Ou, Y., Pang, J., Yang, H., Huang, Q., Chen, S., Zhang, Z., Xu, Y., Cai, Y., Liang, M., Zhang, X., Lai, L., Zheng, Y., 2014. SIRT1 expression in the cochlea and auditory cortex of a mouse model of age-related hearing loss. Exp. Gerontol. 51, 8–14.
Xiong, H., Ou, Y., Xu, Y., Huang, Q., Pang, J., Lai, L., Zheng, Y., 2017. Resveratrol promotes recovery of hearing following intense noise exposure by enhancing cochlear SIRT1 activity. Audiol. Neurootol. 22, 303–310.
Xiong, H., Pang, J., Yang, H., Dai, M., Liu, Y., Ou, Y., Huang, Q., Chen, S., Zhang, Z., Xu, Y., Lai, L., Zheng, Y., 2015. Activation of miR-34a/SIRT1/p53 signaling contributes to cochlear hair cell apoptosis: implications for age-related hearing loss. Neurobiol. Aging 36, 1692–1701.
Yamasoba, T., Lin, F.R., Someya, S., Kashio, A., Sakamoto, T., Kondo, K., 2013. Current concepts in age-related hearing loss: epidemiology and mechanistic pathways. Hear. Res. 303, 30–38.
Yans, A., Shahamati, S.Z., Maghsoudi, A.H., Maghsoudi, N., 2015. Digitoflavone provokes mitochondrial biogenesis in PC12 cells: a protective approach to oxidative stress. Pharm. Biol. 53, 1727–1734.
Ye, X., Sun, X., Starovoytov, V., Cai, Q., 2015. Parkin-mediated mitophagy in mutant hAPP neurons and Alzheimer's disease patient brains. Hum. Mol. Genet. 24, 2938–2951.
Zaini, M.A., Muller, C., de Jong, T.V., Ackermann, T., Hartleben, G., Kortman, G., Guhrs, K.H., Fusetti, F., Kramer, O.H., Guryev, V., Calkhoven, C.F., 2018. A p300 and SIRT1 regulated acetylation switch of C/EBPalpha controls mitochondrial function. Cell Rep. 22, 497–511.
Zhang, Q., Liu, H., McGee, J., Walsh, E.J., Soukup, G.A., He, D.Z., 2013. Identifying microRNAs involved in degeneration of the organ of corti during age-related hearing loss. PLoS One 8, e62786.
Zhong, Y., Hu, Y., Peng, W., Sun, Y., Yang, Y., Zhao, X., Huang, X., Zhang, H., Kong, W., 2012. Age-related decline of the cytochrome c oxidase subunit expression in the auditory cortex of the mimetic aging rat model associated with the common deletion. Hear. Res. 294, 40–48.
Zhu, J., Wang, K.Z., Chu, C.T., 2013. After the banquet: mitochondrial biogenesis, mitophagy, and cell survival. Autophagy 9, 1663–1676.